

# TiN/Al<sub>2</sub>O<sub>3</sub> composites and graded laminates thereof consolidated by spark plasma sintering

Zhijian Shen\*, Mats Johnsson, Mats Nygren

*Department of Inorganic Chemistry, Arrhenius Laboratory, Stockholm University, 106 91 Stockholm, Sweden*

Received 15 March 2002; received in revised form 5 July 2002; accepted 14 July 2002

## Abstract

A rapid consolidation process named Spark Plasma Sintering (SPS) has been applied to compact duplex TiN/Al<sub>2</sub>O<sub>3</sub> composites and graded laminates thereof. Fully or nearly fully compacted samples were prepared at 1500 °C with a holding time of 3 min under a pressure of 75 MPa. The unusually high grain-growth rate of Al<sub>2</sub>O<sub>3</sub> occurring in monolithic Al<sub>2</sub>O<sub>3</sub> at this sintering temperature is prevented by the addition of TiN particles. Crack-free graded laminates with distinct interfaces between layers were prepared by loading samples inside the die, both symmetrically and asymmetrically. The observed mechanical properties, e.g. hardness and fracture toughness, are related to the microstructural features of the compacted samples.

© 2002 Elsevier Science Ltd. All rights reserved.

*Keywords:* Al<sub>2</sub>O<sub>3</sub>; Composite; Nitrides; Sintering; SPS; TiN

## 1. Introduction

Titanium nitride (TiN) has a high melting point (2950 °C), and exhibits high chemical stability as well as a low friction coefficient in contact with ferrous and nickel based alloys. It has high thermal conductivity,  $21 \pm 1 \text{ W}\cdot\text{m}^{-1}\cdot\text{K}^{-1}$ . Its hardness increases with decreasing grain size, both for polycrystalline bulk materials and for thin films: hardness values of 17.2 and 45 GPa have been reported for a coarse-grained bulk material and for a nano-structured film, respectively.<sup>1</sup> Such a combination of properties makes TiN a potential candidate material for wear-resistant components and cutting-tool inserts. The inherent low damage tolerance of TiN has been shown to be effectively improved by addition of a second phase, e.g. Al<sub>2</sub>O<sub>3</sub>. Thus, a TiN matrix composite reinforced by approximately 40 vol.% dispersed Al<sub>2</sub>O<sub>3</sub> particles was both hard and strong ( $H_v \approx 20 \text{ GPa}$ ,  $\sigma_f \approx 1000 \text{ MPa}$ ) and had a cutting-tool performance comparable to that of cubic boron nitride (c-BN) sintered tools.<sup>2</sup>

TiN is also a good electrical conductor with a room-temperature resistivity of  $3.34 \cdot 10^{-7} \text{ } \Omega \text{ cm}$ .<sup>3</sup> When dis-

persed in a non-conducting matrix the TiN particles not only improve the stiffness and fracture toughness but also the electrical conductivity of the material. Depending on the amount of TiN particles added and on the type of TiN sub-network formed in the composite, specific electrical resistances between 1 and 100  $\mu\Omega \text{ cm}$  have been obtained for TiN–Al<sub>2</sub>O<sub>3</sub> composites. This suggests that such composites can be used as electrical heaters and heat exchangers, and that composite components of complex shape can be manufactured by electrical discharge machining.<sup>4–6</sup>

The aim of the present work was to evaluate the applicability of the spark plasma sintering (SPS) technique in compacting duplex TiN/Al<sub>2</sub>O<sub>3</sub> composites and in compacting multi-layered graded structures of TiN/Al<sub>2</sub>O<sub>3</sub> compositions. The mechanical properties, hardness ( $H_v$ ) and fracture toughness ( $K_{1C}$ ), were investigated and correlated with the microstructure and composition, as well as with the preparation conditions used.

SPS is a comparatively new sintering technique. It is similar to conventional hot pressing in a way that the precursors are loaded in a die and a uniaxial pressure is applied during sintering. However, instead of using an external heating source, a pulsed direct current is allowed to pass through the electrically conducting pressure die and, in appropriate cases, also through the

\* Corresponding author. Tel.: +46-8-162388; fax: +46-8-152187.  
E-mail address: shen@inorg.su.se (Z. Shen).

sample. This implies that the die also acts as a heating source and that the sample is heated from both outside and inside. Besides, an external electrical field setting up plays an important role in enhancing mass-transportation. A unique feature of SPS process is thus to enable reaction and consolidation to occur at comparatively lower temperature in a rapid manner.<sup>7,8</sup>

## 2. Experimental

Appropriate amounts of TiN (H.C. Starck-Berlin, grade C) and  $\alpha$ -Al<sub>2</sub>O<sub>3</sub> (Ceralox APA-0.5) powders, with

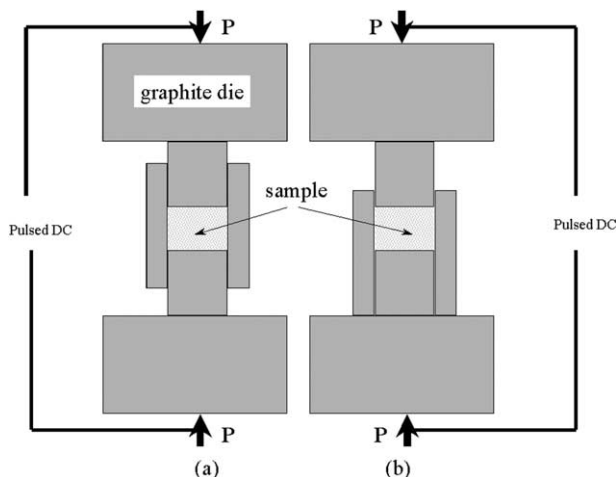


Fig. 1. Schematic diagrams illustrating (a) the symmetrical and (b) asymmetrical loading of precursor powders inside the graphite pressing die.

average particle sizes of 1.0 and 0.4  $\mu\text{m}$ , respectively, were mixed in a high-speed planetary mill with water-free 2-propanol as liquid medium, to yield a series of TiN–Al<sub>2</sub>O<sub>3</sub> mixtures with TiN vol.% of 0, 20, 40, 50, 60, 80, and 100. The dried powder mixtures were consolidated in vacuum in an SPS apparatus (Dr. Sinter 2050, Sumitomo Coal Mining Co. Ltd., Japan), using a cylindrical graphite die with an inner diameter of 20 mm. The sintering temperature was set at 1500 °C with a holding time of 5 min. A pressure of 75 MPa was applied at room temperature and released at the end of the holding time. The temperature was automatically raised to 600 °C, from there onwards it was monitored and regulated by an optical pyrometer focused on the surface of the die. A heating rate of 100 °C·min<sup>-1</sup> between 600 and 1500 °C was used for all the materials. The set-up allows a cooling rate of > 350 °C·min<sup>-1</sup> from the sintering temperature down to 1000 °C.

Each layer in the laminates was about 0.5 mm thick, and Al<sub>2</sub>O<sub>3</sub> was always placed at the bottom of the die, followed by five layers of TiN–Al<sub>2</sub>O<sub>3</sub> powder mixtures with progressively increasing TiN content and, finally, a layer of pure TiN, thus giving a structure consisting of seven layers.

The laminated precursors were loaded into the graphite die in two different ways: symmetrical or asymmetrical. With the symmetrical loading, as illustrated in Fig. 1a, the temperature distribution is homogeneous, whereas an asymmetrical loading of the sample, as illustrated in Fig. 1b, gives rise to a temperature gradient inside the die, i.e. the temperature is lower at the bottom punch than at the top, because the current density in the upper

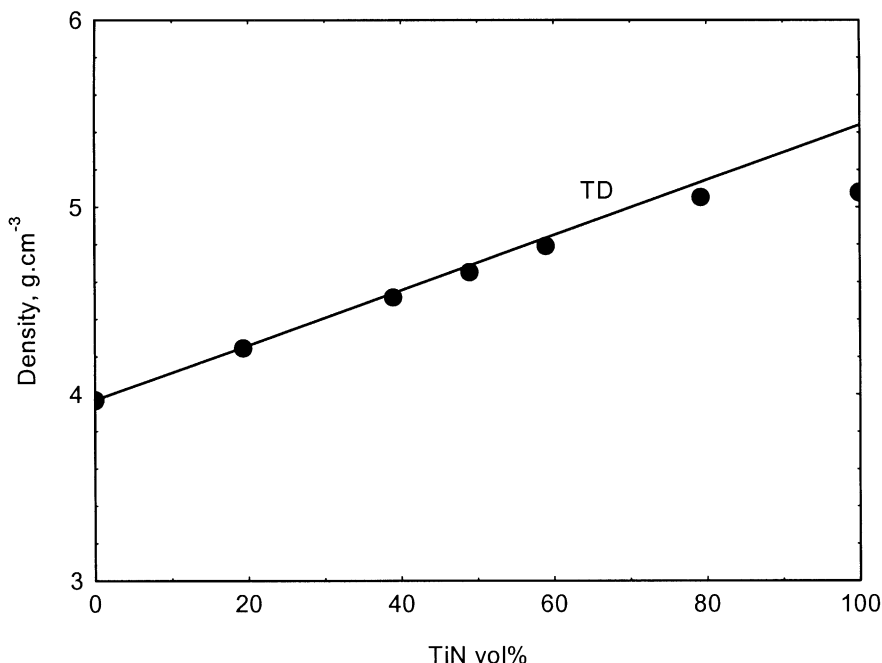


Fig. 2. Measured density values plotted versus compositions for duplex TiN/Al<sub>2</sub>O<sub>3</sub> composites.

punch is higher than in the lower one. The duplex TiN/ $\text{Al}_2\text{O}_3$  composites were all loaded symmetrically.

The density of the compacted specimens was measured according to Archimedes' principle. The specimens were carefully polished by standard diamond polishing techniques down to 1  $\mu\text{m}$  finish. The hardness ( $H_v$ ) and indentation fracture toughness ( $K_{Ic}$ ) were measured at room temperature by the Vickers diamond indentation method and evaluated by the equations given by Evans

et al.<sup>9</sup> The microstructure was investigated in scanning electron microscopes (SEM, Jeol 820 and 880), both equipped with energy-dispersive spectrometers (EDS, LINK *ISIS*). In order to obtain the best contrast between different phases, the specimens were thermally etched for 30 min in nitrogen atmosphere at 1300–1350  $^\circ\text{C}$ , and the micrographs were recorded in back-scattered electron mode (BSE). The reported grain sizes are determined based on a linear intercept method.<sup>10</sup>

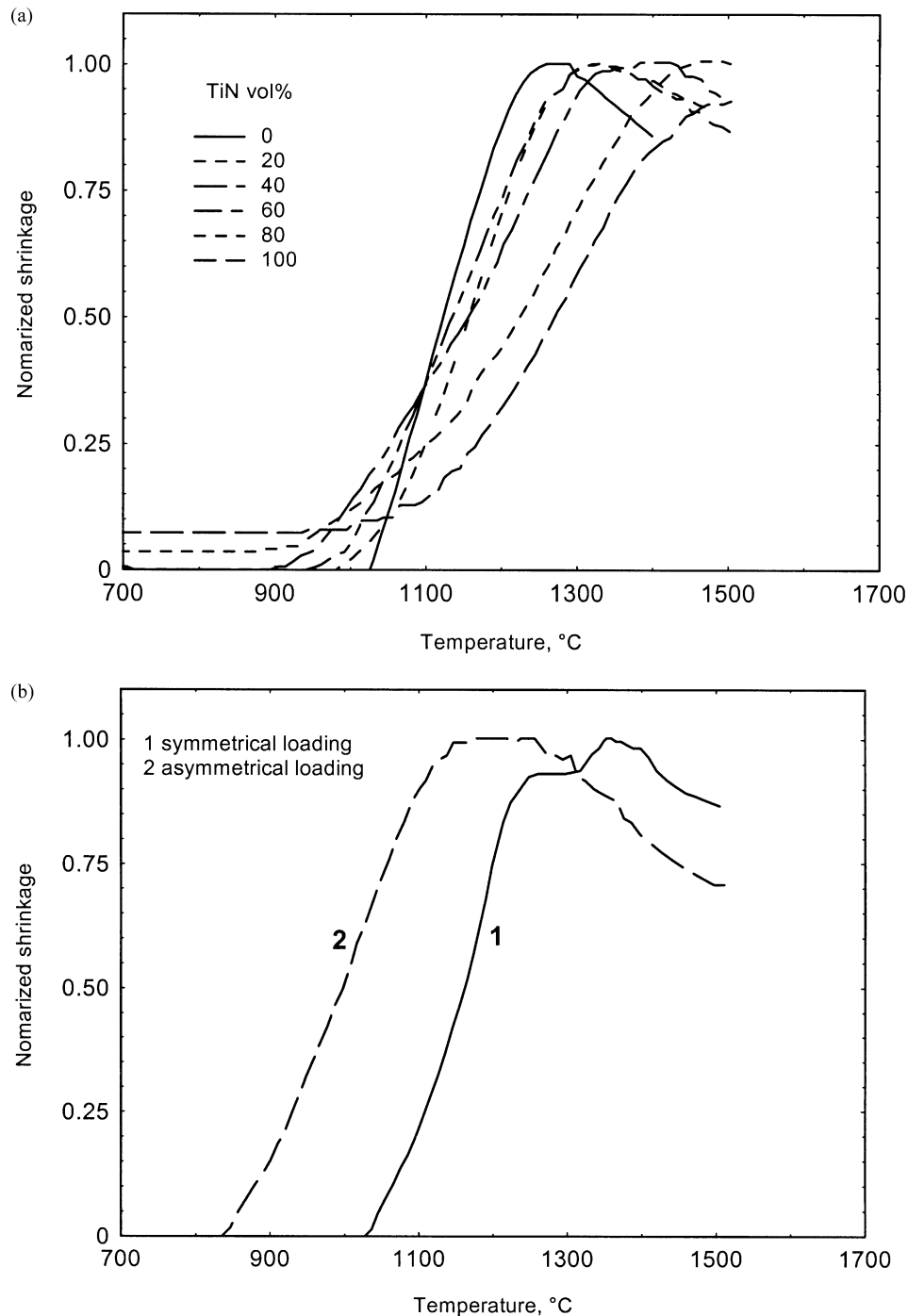


Fig. 3. Normalized shrinkage of (a) individual duplex TiN/ $\text{Al}_2\text{O}_3$  composites and (b) graded laminates during SPS compacting.

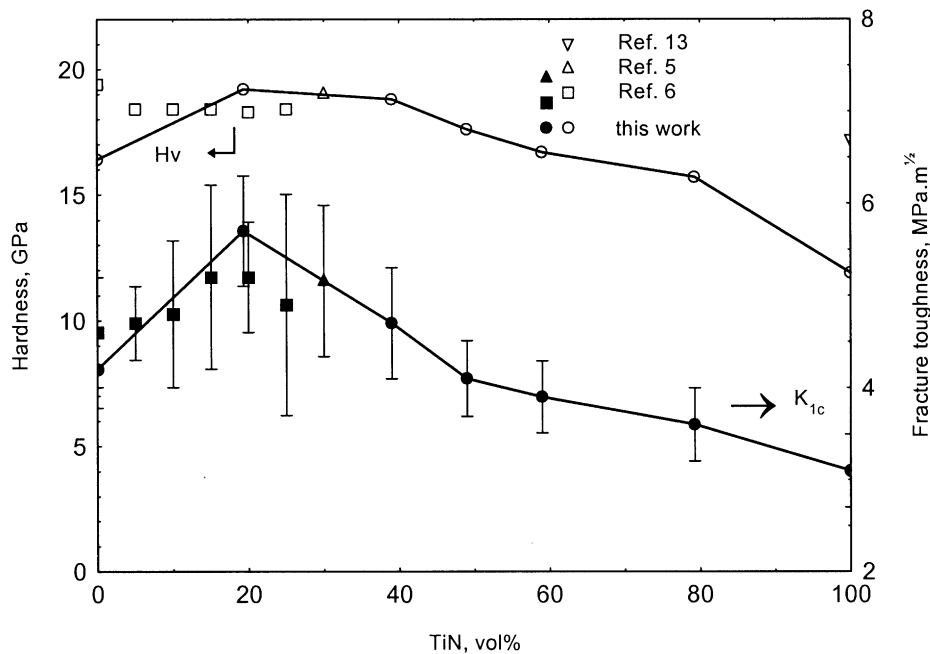


Fig. 4. Hardness and indentation fracture toughness versus TiN content for duplex TiN/Al<sub>2</sub>O<sub>3</sub> composites. Data from Refs. 5, 6, 13 are included for comparison.

### 3. Results and discussion

#### 3.1. Densification

The measured density values of the compacted bodies are plotted versus their compositions in Fig. 2. The used sintering conditions yielded densities corresponding to 99–100% of the theoretical values (TD) calculated by the rule of mixture for composites containing up to 60 vol.% TiN, while pure TiN reached only ~95% TD.

Typical shrinkage curves during sintering of the TiN/Al<sub>2</sub>O<sub>3</sub> composites are given in Fig. 3. It is obvious that a higher sintering temperature is required for densifying TiN than for Al<sub>2</sub>O<sub>3</sub>. The shrinkage of TiN is not finished at 1500 °C, while for Al<sub>2</sub>O<sub>3</sub> it is finished already at 1290 °C; the subsequently observed negative shrinkage is due to the thermal expansion of the graphite die. For the composite materials, the densification temperature increases with the increase of TiN content, and the shape of the sintering curves reveals that they are homogeneously densified, see Fig. 3a. However, the shrinkage curve of the symmetrically loaded laminated composite shows that densification takes place in two steps, see curve 1 in Fig. 3b. It is tempting to interpret this behavior in terms of the alumina-rich layers being densified in the low-temperature region and the TiN-rich ones in the high-temperature region. However, when the layered structure is asymmetrically loaded, the densification seems to take place in one step, see curve 2 in Fig. 3b. It can also be noted that the densification in the latter case is finished at a “lower temperature” than in the former case. Certainly, this does not imply that the

material is easier to compact in the latter case; it rather exemplifies the experimental difficulty associated with measurements of actual temperatures inside the die. According to our and other workers experience with compacting metallic and non-metallic powder mixtures by the SPS technique, the temperature inside the die, in symmetrically loaded samples, is ~75 °C higher than that recorded outside. By comparing the two shrinkage curves given in Fig. 3b, it seems plausible to assume that in the asymmetric case the temperature of the upper part of the laminate structure is ~150 °C higher than that of the lower part.

The measurements show that the TiN/Al<sub>2</sub>O<sub>3</sub> composites become more difficult to sinter with increasing fraction of TiN. The density values obtained in the present study are very much the same as those obtained for hot-pressed (HP) or hot isostatically pressed (HIP) samples sintered in the temperature range 1650–1750 °C,<sup>2,5,6,11</sup> while the entire processing time required for SPS is less than 1/10 of that required in the HP and HIP processes. It thus seems appropriate to conclude that SPS is an efficient process for consolidating this family of composite materials.

#### 3.2. Mechanical properties and microstructures of the TiN/Al<sub>2</sub>O<sub>3</sub> composites

The measured values of the hardness and indentation fracture toughness are plotted in Fig. 4 versus the TiN content of the TiN/Al<sub>2</sub>O<sub>3</sub> composites. The general tendency is that the composite materials containing 20–40 vol.% TiN are harder than monolithic Al<sub>2</sub>O<sub>3</sub>. The fracture

toughness of the composites increases with the addition of TiN, presents a maximum value,  $5.7 \text{ MPa m}^{1/2}$ , at 20 vol.% TiN, then decreases with the further increase of TiN content. These observations are in good agreement with previous findings for hot-pressed TiN/Al<sub>2</sub>O<sub>3</sub> composites.<sup>2,5,6</sup> The monolithic TiN and composites with TiN content larger than 50 vol.% had lower hardness and fracture toughness values than expected, due to its low density. Al<sub>2</sub>O<sub>3</sub> can be compacted at much lower temperatures than 1500 °C by the SPS technique, and the hardness increases with decreasing grain size.<sup>9</sup>

Accordingly, the monolithic Al<sub>2</sub>O<sub>3</sub> ceramics prepared in this study have very coarse microstructures, containing grains larger than 10 μm in size, as seen in Fig. 5. The addition of TiN effectively inhibits the grain growth of Al<sub>2</sub>O<sub>3</sub>. In composites containing 20 vol.% TiN, the grain size of Al<sub>2</sub>O<sub>3</sub> is thus reduced to about 2 μm, and with increasing amount of TiN the grain size of Al<sub>2</sub>O<sub>3</sub> is

further reduced to less than 1 μm, e.g. only twice the size of the precursor powder. The grain growth of TiN is not as dramatic as that of Al<sub>2</sub>O<sub>3</sub>. The average grain size in the TiN compact prepared at 1500 °C is ~2 μm, compared to 1 μm in the starting powder. The wide size distribution of the TiN particles was almost the same in all TiN/Al<sub>2</sub>O<sub>3</sub> composites, i.e. in the 0.2–2 μm range.

Previous studies of SPS-compacted Al<sub>2</sub>O<sub>3</sub> have shown that the hardness increases with decreasing grain size.<sup>12</sup> A compact prepared at 1250 °C from the same precursor powder as in this study, and having an average grain size of 1 μm, exhibited a hardness value of ~20 GPa. It is therefore tempting to ascribe the hardness increase of compacts containing less than 40 vol.% TiN to decreasing grain size of Al<sub>2</sub>O<sub>3</sub> rather than to the previously accepted explanation that TiN is stiffer and harder than the Al<sub>2</sub>O<sub>3</sub> matrix. In fact, assuming that the Al<sub>2</sub>O<sub>3</sub> matrix has a hardness value of 20 GPa, and using

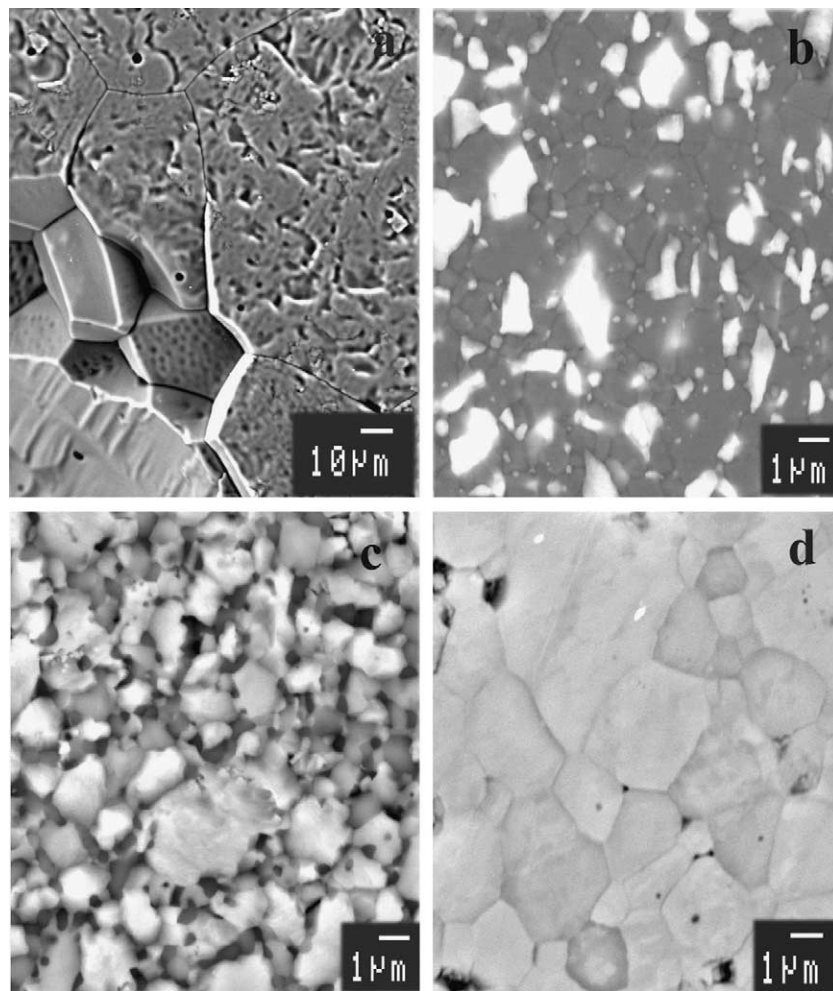


Fig. 5. SEM micrographs of TiN/Al<sub>2</sub>O<sub>3</sub> composites recorded in back-scattered electron mode, with (a) 0 vol.%, (b) 20 vol.%, (c) 80 vol.%, and (d) 100 vol.% TiN, respectively.

measured data for the samples containing 20% and 40 vol.% TiN, application of the linear mixing rule yields a hardness value of  $\sim 18$  GPa for the pure TiN compact. This is in good agreement with data reported for a polycrystalline TiN bulk material with similar grain size.<sup>13</sup> This interpretation implies that the hardness actually decreases with increasing TiN content in the present case. However, bulk compacts of TiN containing submicron- to nano-sized grains are reported to have hardness values above 22 Gpa,<sup>1</sup> implying that if corresponding  $\text{Al}_2\text{O}_3/\text{TiN}$  composites are prepared with nano- instead of micron-sized TiN particles, the hardness of these composites might be even higher than that of monolithic  $\text{Al}_2\text{O}_3$ . The drop of the hardness and toughness above 50 vol.% TiN is not representative, it is most probably mainly due to the presence of remained pores. Investigations of the propagation route of the Vicker's indentation cracks reveal that the cracks mainly propagate intergranularly in all composites prepared. It is thus reasonable to assume that the predominating toughening mechanism is related to crack tilting and twisting caused by thermal expansion and/or elastic modulus mismatch stresses.

As mentioned above, the grain growth rate of  $\text{Al}_2\text{O}_3$  is greatly enhanced by increasing the SPS processing temperature, and in this respect 1500 °C is very high. This causes problems when compacting composite precursor powder mixtures that are not well dispersed, i.e. which contain aggregates of  $\text{Al}_2\text{O}_3$ . In such cases comparatively large  $\text{Al}_2\text{O}_3$  grains are formed, as seen Fig. 6. From a mechanical point of view, these large grains give rise to detrimental flaws and depress the strength of the compact. It can be noted that inside these aggregates the grains adjust their growth direction to form clean crystallographic surface boundaries, while randomly oriented surfaces are formed at the borders towards the matrix.

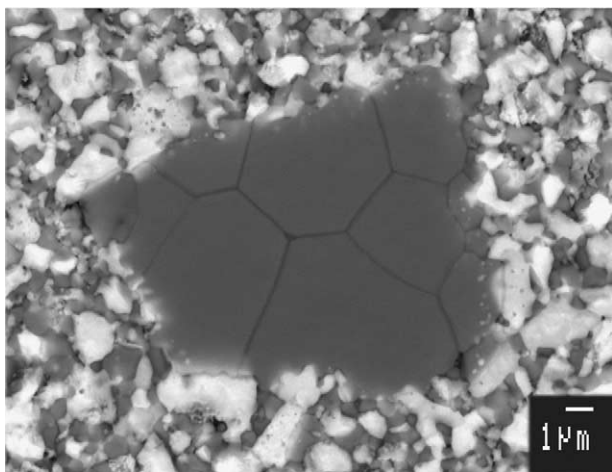


Fig. 6. Abnormal grain growth of  $\text{Al}_2\text{O}_3$  inside an aggregate in the sample consisting of 60 vol.% TiN.

### 3.3. Mechanical properties and microstructures of the graded laminates

Crack-free laminates composed of seven layers containing 0, 20, 40, 50, 60, 80, 100 vol.% TiN, each having a thickness of around 0.5 mm, were obtained after being SPSed at 1500 °C for 5 min, using a pressure of 75 MPa, both for symmetrically and asymmetrically loaded samples. A back-scattered SEM micrograph of one of these composites is shown in Fig. 7. The existence of distinct interfaces between layers is obvious. Under high magnification it becomes clear that the microstructure of each layer resembles the corresponding composite discussed above, see Fig. 8.

The hardness values determined within each layer are given in Fig. 9, which decreases gradually from the layer containing 20 vol.% TiN to the one containing 100 vol.% TiN, in fair agreement with the findings for the composite materials. The hardness value of the pure  $\text{Al}_2\text{O}_3$  layer is lower than expected, due to its coarse-grained structure. It is difficult to evaluate the density of

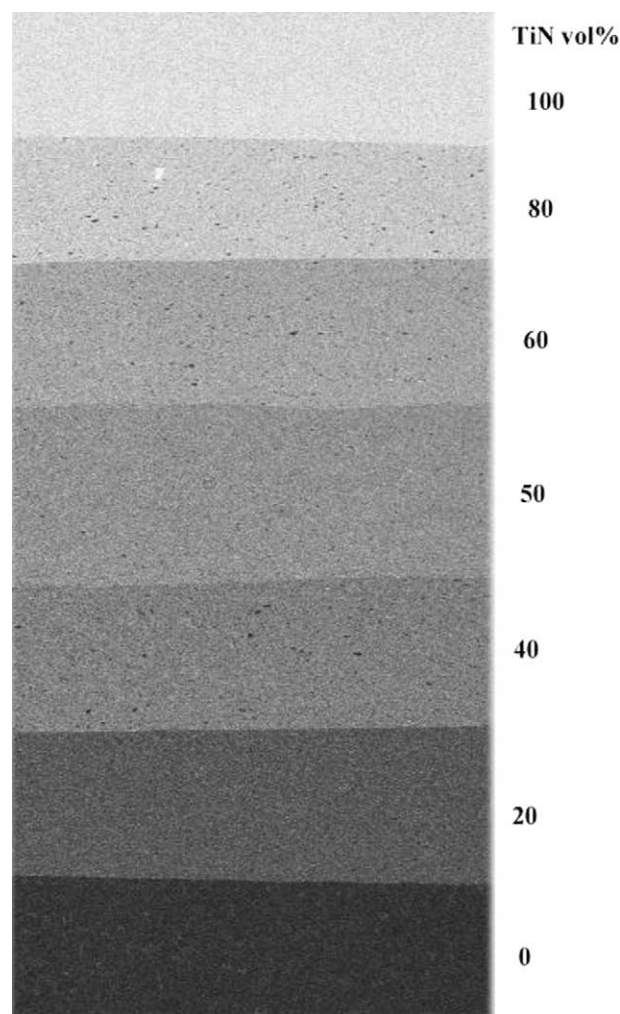


Fig. 7. Low-magnification back-scattered SEM micrograph of the graded laminates composed of seven layers.

the individual layers inside the laminates, but from the determined hardness values and inspection of obtained SEM micrographs it can be estimated that all the layers are fully densified, except for the pure TiN layer. Even if the pure TiN layer has not reached full density it seems to be denser than the monolithic TiN compact, especially when the sample is loaded in the asymmetrical mode, as indicated both by SEM observations and the measured hardness values. In the latter case, the TiN layer contains larger grains than in the former, suggesting that it has been exposed to a temperature higher than 1500 °C, see also above.

The fact that no crack is observed indicates the low residual stress level inside the laminates. One origin of residual stress is the thermal expansion mismatch of the different phases involved. In the present case, the thermal expansion coefficients of Al<sub>2</sub>O<sub>3</sub> and TiN are very

similar, with reported values of  $8.0\text{--}9.1\cdot 10^{-6}$  and  $8.0\text{--}9.3\cdot 10^{-6}$  for Al<sub>2</sub>O<sub>3</sub> and TiN, respectively.<sup>5,6,14</sup> One may therefore expect that the residual stress initiated by thermal-expansion mismatch should be small in this type of laminated structure. However, when pure Al<sub>2</sub>O<sub>3</sub> and TiN were laminated alternately to form a laminated composite, cracks easily developed perpendicular to the Al<sub>2</sub>O<sub>3</sub>/TiN interfaces during polishing of the sample, see Fig. 10, indicating that high residual tensile stresses were built up inside the TiN layers. As shown in Fig. 3a, TiN reaches only ~50% of normalized shrinkage at the temperature where Al<sub>2</sub>O<sub>3</sub> is fully densified. The early densified Al<sub>2</sub>O<sub>3</sub> layers may thus restrain further shrinking of TiN during the later part of sintering, so that tensile stresses build up within the TiN layers. Such a way of producing residual stress in laminated composites is probably more essential than thermal-expansion mismatch in the present system. In a compositional-gradient laminate the densification temperatures of neighboring layers are closer together, therefore the residual stresses built up inside the layers are reduced. This becomes even more obvious when the compositional-gradient laminate is asymmetrically loaded; so that different layers are compacted simultaneously due to a temperature-field gradient set up inside the die, see Fig. 3b. Consequently, the residual stresses inside the laminate prepared are further reduced. One indication of this difference is the crack propagation straight through the layer interfaces in the asymmetrically loaded laminate, compared to the slight deflection at the interfaces in the symmetrically loaded laminate.

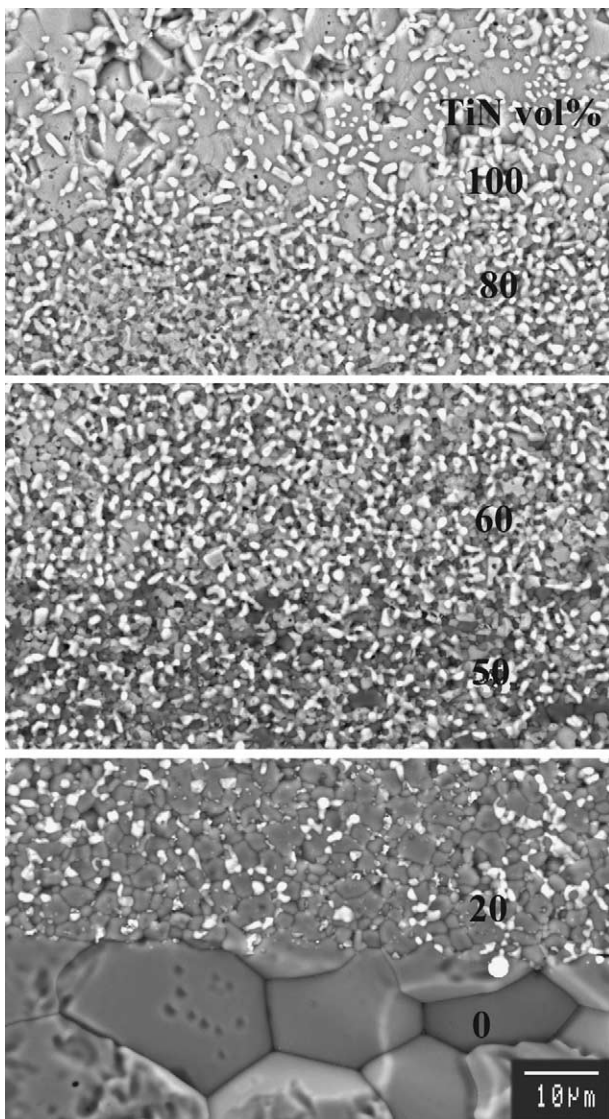


Fig. 8. SEM micrographs of the interfaces between selected layers in an asymmetrically loaded functional gradient composite.

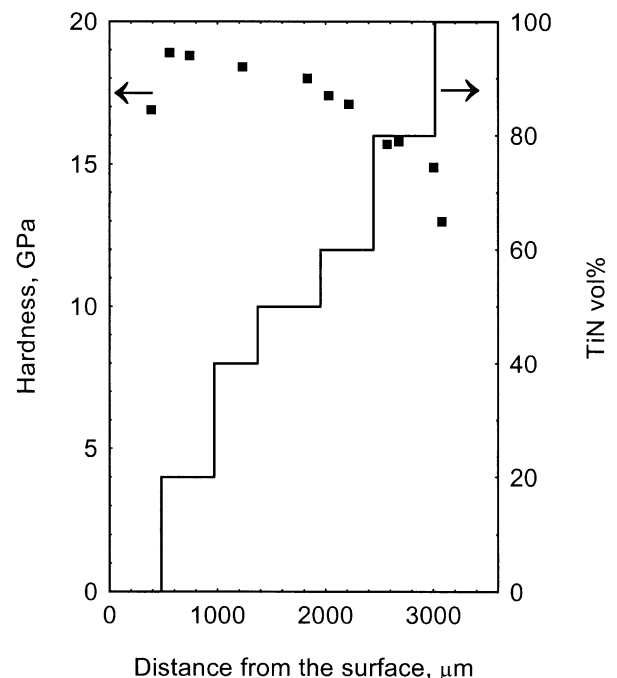


Fig. 9. The hardness across layers in a graded laminate.

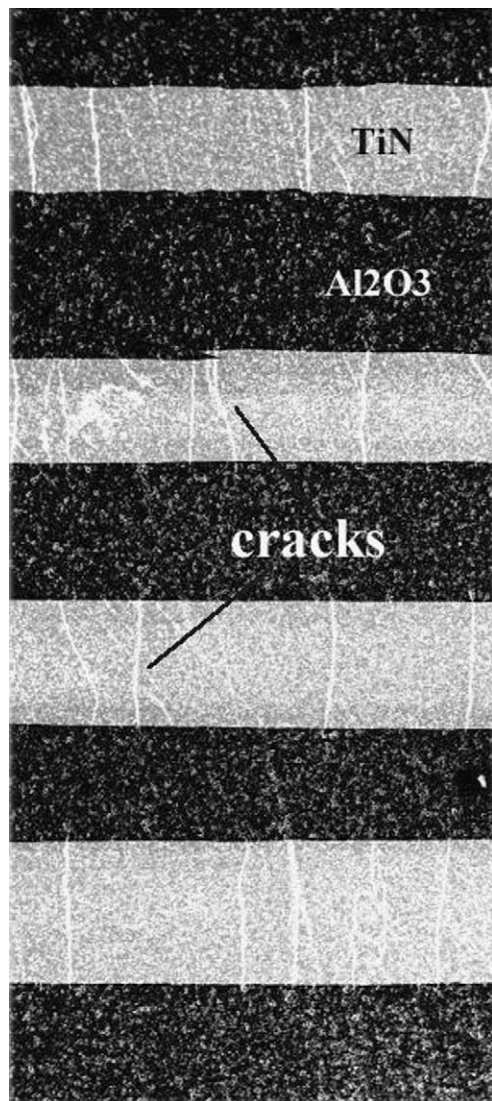


Fig. 10. Cracks formed inside the TiN layers when pure  $\text{Al}_2\text{O}_3$  and TiN are alternately laminated.

#### 4. Concluding remarks

It is shown that the SPS process can be applied to consolidate TiN/ $\text{Al}_2\text{O}_3$  composites and graded laminates thereof in absence of any additives. The entire processing time required for obtaining fully densified composites is less than 1/10 of that required by conventional sintering processes. The monolithic  $\text{Al}_2\text{O}_3$  ceramics prepared in this study exhibit very coarse microstructures, whereas the addition of TiN effectively inhibited the grain growth of  $\text{Al}_2\text{O}_3$ . Crack-free laminates composed of seven layers containing 0, 20, 40, 50, 60, 80, 100 vol.% TiN, each with a thickness of around 0.5 mm, were prepared both with symmetrically and asymmetrically loaded samples. The existence of distinct interfaces between layers was noticed. The microstructure of each layer resembles that of the corre-

sponding composite. The hardness decreases gradually from the layer containing 20 to that containing 100 vol.% TiN, in fair agreement with the findings for the composites. SEM studies suggest that all layers except the pure TiN layer are fully dense. The difference between the densification rates of TiN and  $\text{Al}_2\text{O}_3$  introduces residual stresses when the two components alternate in laminated composites. Making a laminated compositional-gradient structure, especially when the laminate is asymmetrically loaded, can reduce this type of residual stress.

#### Acknowledgements

This work was supported by the Swedish National Board for Industrial and Technical Development (NUTEK).

#### References

- Andrievski, R. A., Nanocrystalline bodies and related compounds. *J. Solid State Chem.*, 1997, **133**, 249–253.
- Egawa, T., Ichikizaki, T., Tsukamoto, H., Tsunoda, H. and Shimoyama, T., Material characteristics and cutting performance of TiN- $\text{Al}_2\text{O}_3$  ceramic tool. *Int. J. Jpn. Soc. Precis. Eng.*, 1995, **29**(3), 222–228.
- Gogotsi, Y. G. and Porz, F., Mechanical properties and oxidation behaviour of  $\text{Al}_2\text{O}_3$ -TiN composites. *J. Am. Ceram. Soc.*, 1992, **78**, 2251–2259.
- Winter, V., Knitter, R., Miniaturization and electric heatability of an  $\text{Al}_2\text{O}_3$ /TiN ceramic composite. In *Werkstoffwoche'98, Band VII: Symp. 9, Keram., Symp. 14, Simul. Keram.* Wiley-VCH Verlag GmbH, 1999, pp. 199–204.
- Bellosi, A., De Portu, G. and Guicciardi, S., Preparation and properties of electrically conductive alumina-based composites. *J. Eur. Ceram. Soc.*, 1992, **10**(4), 307–315.
- Rak, Z. S. and Czechowski, J., Manufacture and properties of  $\text{Al}_2\text{O}_3$ -TiN particulate composites. *J. Eur. Ceram. Soc.*, 1998, **18**(4), 373–380.
- Tokita, M., Trends in advanced SPS spark plasma sintering system and technology. *J. Soc. Powder Technol., Jpn.*, 1993, **30**(11), 790–804.
- Gao, L., Shen, Z., Miyamoto, H. and Nygren, M., Superfast densification of oxide/oxide ceramic composites. *J. Am. Ceram. Soc.*, 1999, **82**(4), 1061–1063.
- Evans, A. G. and Charles, E. A., Fracture toughness determination by indentation. *J. Am. Ceram. Soc.*, 1976, **59**(7–8), 371–372.
- Mendelson, M. I., Average grain size in polycrystalline ceramics. *J. Am. Ceram. Soc.*, 1969, **52**(8), 443–446.
- Yamamoto, R., Murakami, S. and Maruyama, K., High-temperature mechanical properties of hot-pressed TiN with fine grain size. *J. Mater. Sci.*, 1998, **33**, 2047–2052.
- Shen, Z. J., Johnsson, M., Zhao, Z. and Nygren, M., Spark plasma sintering of  $\text{Al}_2\text{O}_3$ . *J. Am. Ceram. Soc.*, 2002, **85**(8), 1921–1927.
- Lengauer, W., Properties of bulk  $\delta$ -titanium nitride ( $\delta$ -TiN<sub>1-x</sub>) prepared by nitrogen diffusion into titanium metal. *J. Alloys Compd.*, 1992, **186**(2), 293–307.
- Oyama, S. T., *The Chemistry of Transition Metal Carbides and Nitrides*. Blackie Academic & Professional, Glasgow, UK, 1996.